JOURNAL OF MATERIALS SCIENCE 26 (1991) 5254–5260

# Thermoelastic martensitic transformation in Cu–Zn–Al alloy

Y. DENG
*University of Science and Technology Beijing, Beijing 100083, People's Republic of China*
G. S. ANSELL
*Colorado School of Mines, Golden, CO 80401, USA*

Thermoelastic martensitic transformation in a Cu–29% Zn–3% Al alloy has been observed with optical and electron microscopy, including 1.0–1.2 MV high-voltage transmission electron microscopy (TEM), and treated with the phenomenological theory suggested before. The observation showed that the transformation was conducted in three stages: parallel plates growing, self-accommodating variants advancing, and plates merging and/or tiny plates forming in carved-up parent phase areas. TEM showed that the martensite consisted of a huge number of packets with constant size and distinct interfaces. By using the phenomenological theory, the free-energy function as well as the friction quasi-enthalpy and friction quasi-entropy are obtained in SI units. Comparing with classical theory, the free energy can be broken into three parts: the chemical free energy, the interfacial energy and the elastic strain energy. In the range of 20–70% martensite in the alloy, the interfacial energy per unit of martensite formation is constant and the corresponding elastic strain energy is a linear function of martensite percentage. Some possible explanations for this energetics relating to the observation are given.

## 1. Introduction

In previous work by the authors [1, 2], electrical resistance measurements showed three stages in the thermoelastic martensitic transformation in Cu–29% Zn–3% Al alloy. From Fig. 5 in Deng and Ansell [1], the transformation slope $dm/dT$ of the cooling process (where $m$ = martensite percentage) can be plotted as in Fig. 1. Then, the transformation can be roughly divided into increasing, constant and decreasing slope stages. This study is a further investigation into the micro-processes corresponding to the three stages, especially the second one. High-voltage transmission electron microscopy (TEM) (1.0–1.2 MV), with a cold stage down to 133 K, has been used among other measures to observe thicker foil morphologies which may be close to those in bulk samples. This investigation would provide some basis for understanding the transformation mechanism and some clues to analysing the elastic strain energy and interfacial energy, both of which are related closely to the shape of the martensite. In order to analyse the free-energy change as well as the elastic strain energy and the interfacial energy, the phenomenological theory suggested before [1, 2] has been used and compared with classical theory [3]. Attention is paid to the relationship between the energetics and the morphology observations.

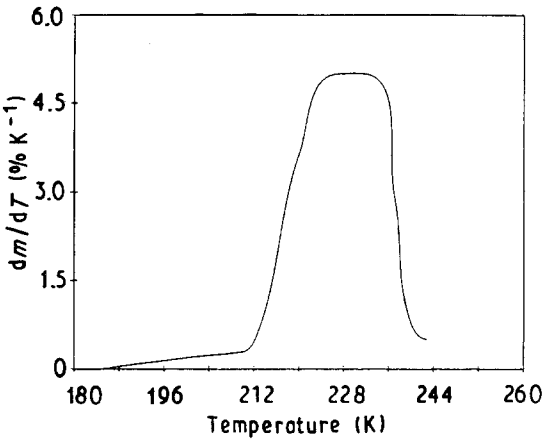


*Figure 1* Three transformation stages shown by the relationship between $dm/dT$ and temperature during cooling.

## 2. Experimental results

### 2.1. First stage of transformation

The details of the sample preparation are described elsewhere [1, 2]. Metallographic samples and TEM foils were cut from single crystals of Cu–29% Zn–3% Al alloy grown by the Bridgman method. Fig. 2 shows the first stage of the transformation on cooling. The transformation started with one variant of parallel martensite plates, and then the second variant appeared and was followed by the third one, and went on. The normal to the sample surface was measured by X-ray diffraction to be (1 1 1) of the parent phase. The horizontal tie-line between the pairs of black



0022–2461/91 $03.00 + .12 

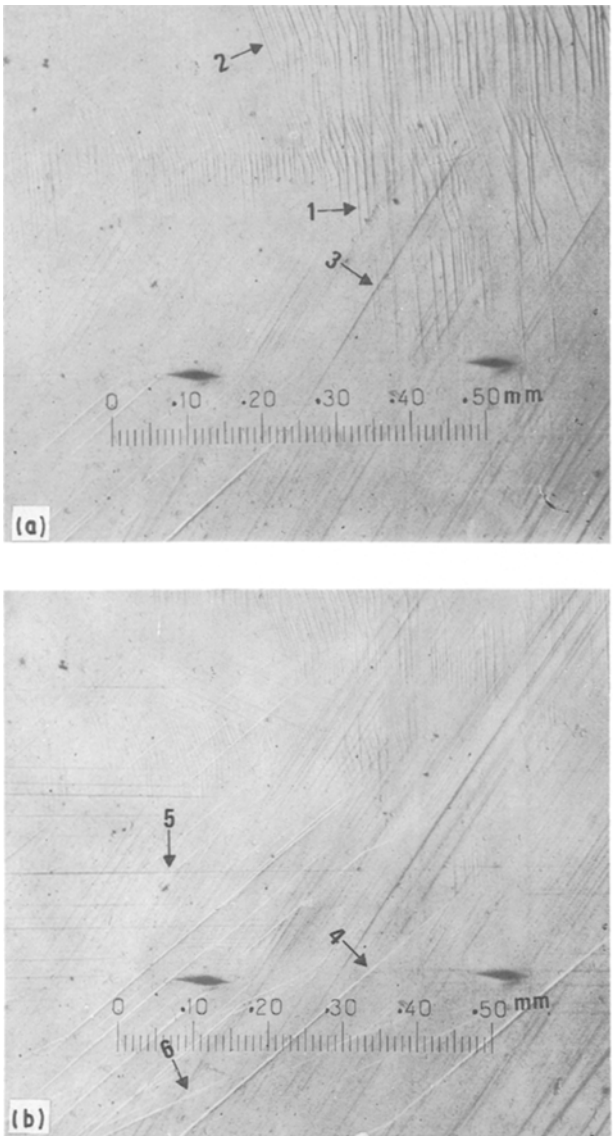


*Figure 2* The sequence of different variants during cooling: (a) 240 K, (b) 237 K.

diamond markers in Fig. 2 is [1 10 9]. The habit plane in the alloy was measured [2] to be the same as in Cu–Zn alloy determined by Schroeder and Wayman [4]. The appearing sequence of the variants and their indices are shown in Table I. This sequence must be related to that of the energy barriers from low to high associated with the different variants.

TABLE I The appearing sequence of variants

| Sequence | Angle $M$[a] (deg) | Habit plane | Trace | Angle $C$[a] (deg) |
|---|---|---|---|---|
| 1st | 90 | $(2\,\bar{1}\,\bar{1}\,12)$ | $[\bar{2}3\,10\,13]$ | 90.9 |
| 2nd | 110 | $(11\,2\,12)$ | $[10\,\bar{1}\,\bar{9}]$ | 109.6 |
| 3rd | 57 | $(11\,12\,\bar{2})$ | $[14\,\bar{1}\,\bar{3}\,\bar{1}]$ | 58.4 |
| 4th | 42 | $(11\,\bar{1}\,\bar{2}\,2)$ | $[\bar{1}\,\bar{4}\,9\,23]$ | 42.4 |
| 5th | 0 | $(2\,11\,12)$ | $[1\,\bar{1}\,0\,9]$ | 0.0 |
| 6th | 22 | $(\bar{1}\,\bar{1}\,2\,12)$ | $[10\,\bar{2}\,\bar{3}\,13]$ | 20.4 |

[a] Angle $M$ is the measured angle between the tie-line of the black diamonds in Fig. 2 and the trace of the martensite in degrees, and angle $C$ is the corresponding calculated angle in degrees.

The radial growth (elongation) of the martensite plate is thermoelastical. That is, during cooling, each temperature corresponded an equilibrium length. Stopping cooling stopped elongating of the plate, and heating led to shrinkage of the length of the plate after a certain hysteresis. Fig. 3 shows the martensite morphology under high-voltage TEM, which can show some features similar to that of bulk samples, i.e. three-dimensional. It can be seen that the shape of the plate is far from oblate spheroidal, which was assumed by some investigators [5, 6]. Moreover, the boundary of the martensite plate is not flat and smooth, but is very rugged.

## 2.2. Second stage of transformation

Fig. 4 shows the characteristics of the second stage. That is, self-accommodating variants formed and advanced between the parallel plates which had developed mainly in the first stage. The transformation rate in this stage is the highest among the three stages. This is qualitatively consistent with the self-accommodating variants advancing which cause the lowest elastic strain energy in the parent phase. A quantitative treatment is given below. Fig. 5 shows the high-voltage TEM morphology of the parallel plates and the initiating region of the self-accommodating variants. In the figure, the top left pattern is a selected-area diffraction (SAD) pattern of the D03 parent phase and the bottom right is an SAD of the martensite. It can be


*Figure 3* Martensite plate morphology under 1.2 MV TEM at 243 K.

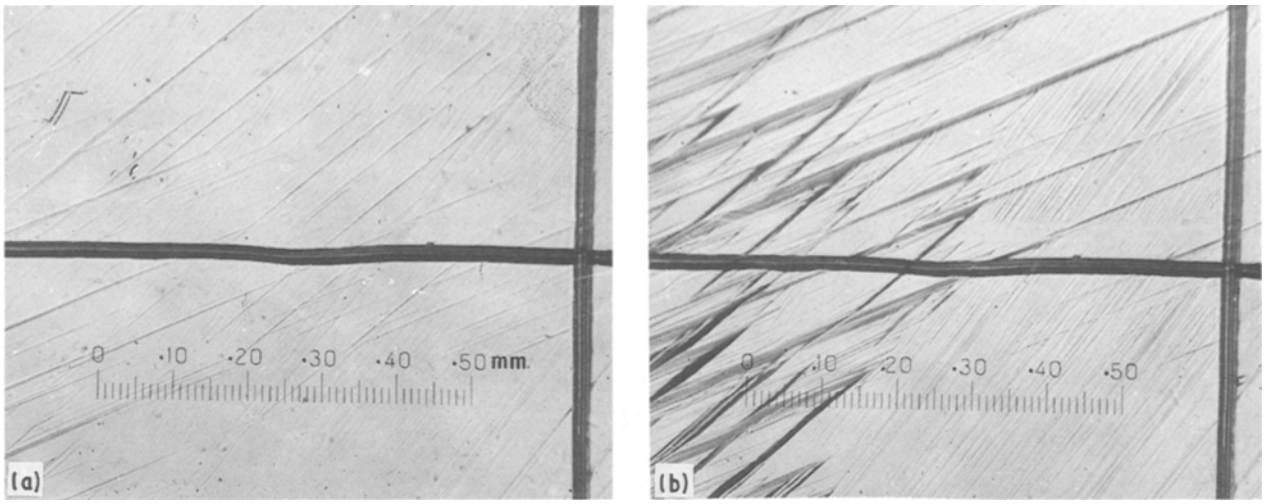


*Figure 4* Self-accommodating variants advancing between parallel martensite plates: (a) 236 K, (b) 228 K.

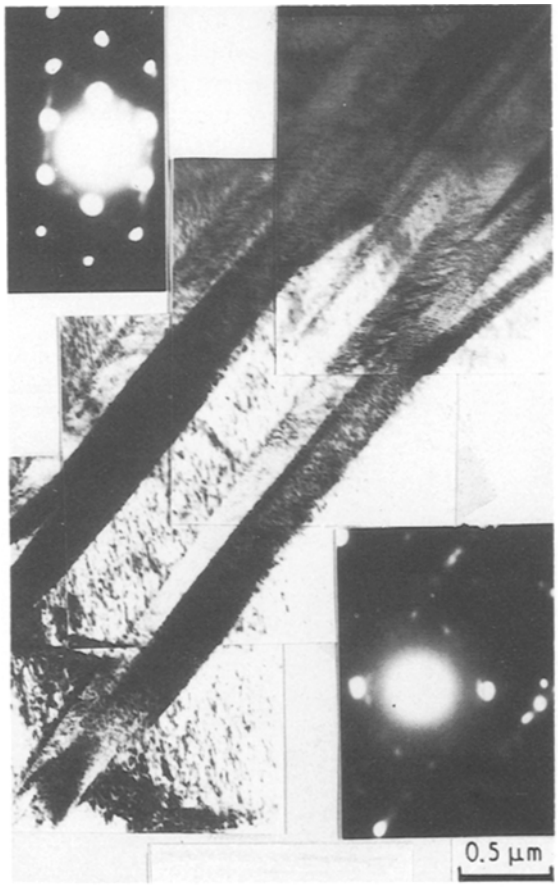


*Figure 5* Martensite morphology under 1.2 MV TEM at 238 K.

seen how the self-accommodating variant plates bifurcate away from the main plate. The main plates are rather like thin laths in shape, as Dunne and Wayman assumed [7]. Furthermore, the growth frontier of the plate is some kind of bifurcated fork in shape. It is noteworthy that in the area of the self-accommodating variants, some parent phase still remained and was carved up further and further by the martensite plates into smaller and smaller areas.

## 2.3. Third stage of transformation

Fig. 6 shows some features of the third stage of the transformation. It seems that two processes are important. First, some parallel plates may merge into one plate. Secondly, in the smaller and smaller parent phase areas carved up by martensite plates, some new and tiny martensite plates nucleated and grew. This constrained growth is further shown by Fig. 7. It can be seen that the tiny plates may be grown in longitudinal orientation (Fig. 7a) or in transversal (Fig. 7b). Both the merging of plates and the growth of tiny plates were conducted in limited and strained spaces, which required higher driving forces for transformation. This explains qualitatively the transformation rate decreasing in the third stage. Fig. 8 shows the final transformed morpholgies without and with a shear stress of 17 MPa on (1 0 1) of the parent phase. Obviously, the transformation was influenced very much by applied stress.

## 2.4. Fine structures in the martensite

Fig. 9 shows the morphology of the martensite over-etched. It can be seen that a martensite plate consists of several sets of a huge number of very tiny packets, just like matchsticks. After over-etching, the individual packets can almost be separated from each other. Fig. 10 shows the morphology under high-voltage TEM. By the high penetrative ability, the stick stack can be seen clearly. The size of the packets is transversely about 10 nm and the length depends on the thickness of the foil. There are obvious interfaces separating the packets. These interfaces and the associated interfacial energy must play some role in the transformation. Fig. 11 shows the boundary dislocations under high-voltage TEM. It can be seen that, besides the dislocation arrays in flat boundaries as reported by Chakravorty and Wayman [8] and Kajiwara and Kikuchi [9], there are dislocation arrays in a sawtooth-shaped boundary.

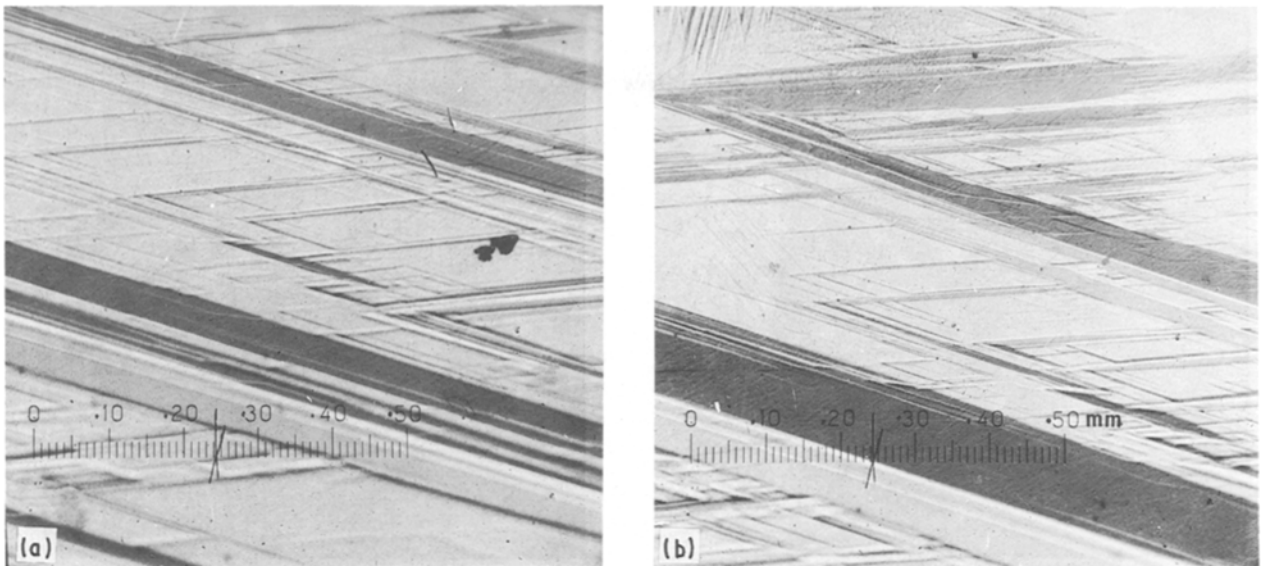


*Figure 6* Martensite merging and new nucleation in carved-up parent phase areas: (a) 213 K, (b) 193 K.

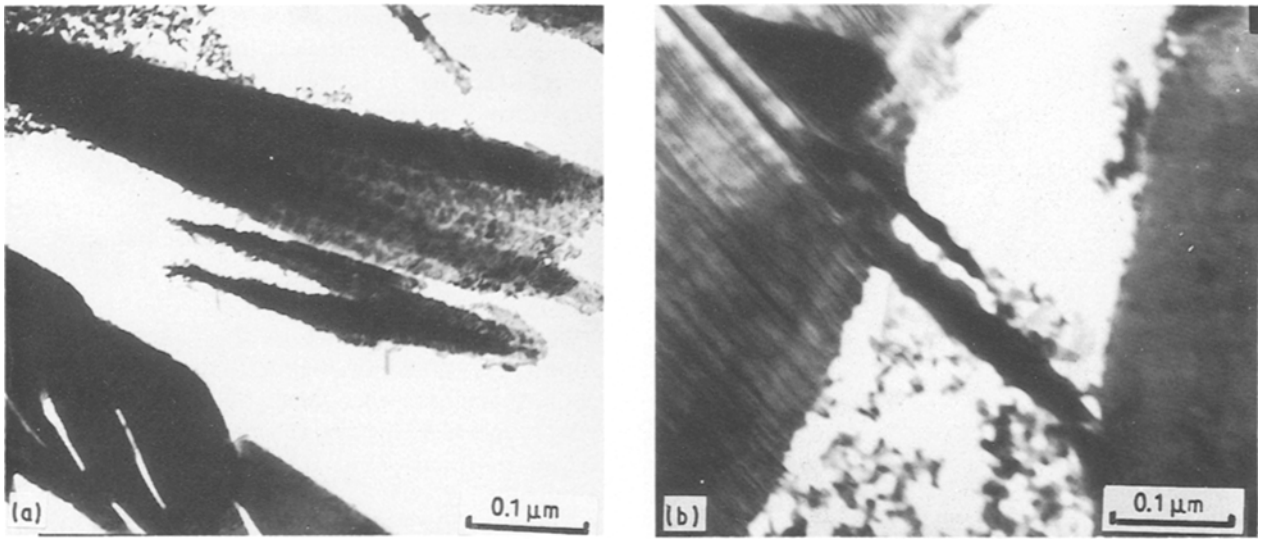


*Figure 7* New tiny martensite plates in carved-up parent phase area: (a) longitudinal, (b) transversal.

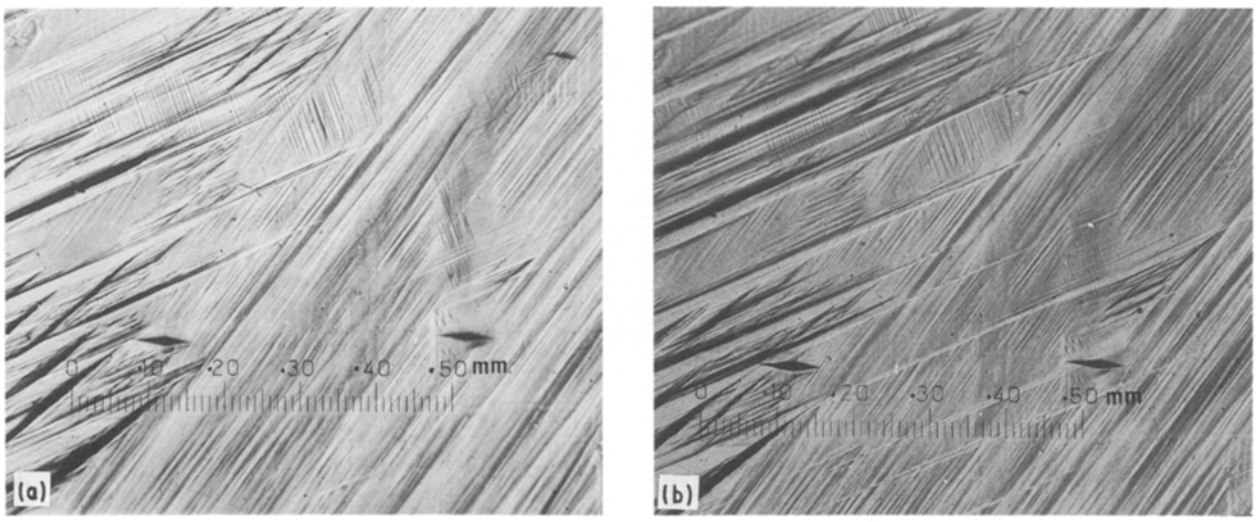


*Figure 8* Final metallography morphology: (a) no stress, (b) with 17 MPa shear stress.


*Figure 9* Martensites consisting of tiny packets.

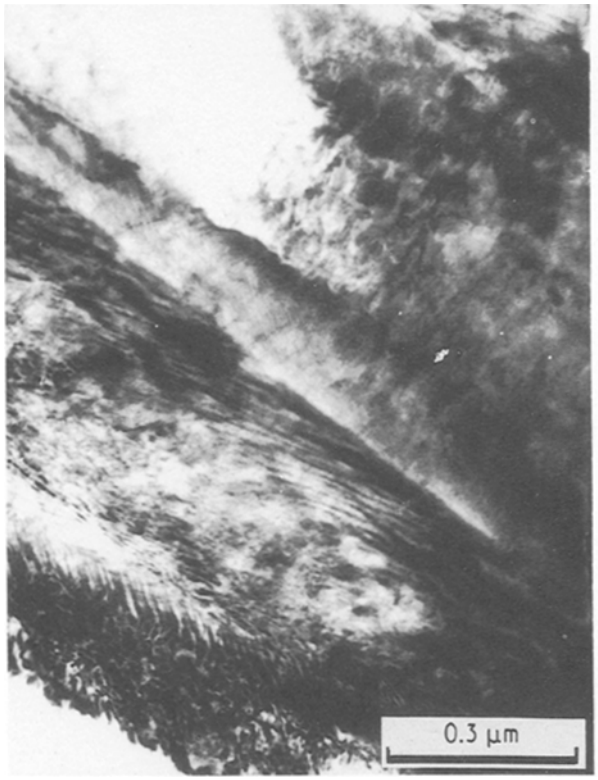


*Figure 10* Martensites consisting of tiny packets under 1.0 MV TEM.

## 3. Theoretical treatment

### 3.1. Free-energy function

The authors have suggested a phenomenological theory for the thermoelastic martensitic transformation in Cu–29% Zn–3% Al alloy [1, 2], in which the free-energy function of the system is

$$F_s = a + bm + cm^2 + e\sigma m \qquad (1)$$

where

$$a = a(T)$$

$$b = 0.064\,51\,T - 15.33$$

$$c = 0.5$$

$$e = 7.393 \times 10^{-5} T - 1.944 \times 10^{-2} \quad (\mathrm{MPa})^{-1}$$


*Figure 11* Martensite boundaries, flat and sawtooth-like, 1.0 MV TEM.

and $m$ is the martensite percentage, and $\sigma$ the applied stress. $F_s$ is a dimensionless free-energy function; in order to convert $F_s$ into the free energy $F_n$ in SI units, the conversion factor $N$ is introduced such that

$$F_n = NF_s \qquad (2)$$

According to classical theory [3], the free-energy change caused by martensitic transformation is

$$\Delta G = G_{ch} + G_{el} + G_{in} \qquad (3)$$

where $G_{ch}$ is chemical free energy change, $G_{el}$ is elastic strain energy and $G_{in}$ is interfacial energy. For one mole of material, when the martensitic transformation percentage is $m$, the free energy of the system is

$$G = G_0 + G_c m + G_e m + G_i m \qquad (4)$$

where $G_0$ is the free energy for 100% parent phase of one mole; $G_c$ is the chemical free energy change caused by one mole of martensitic transformation, $G_e$ is the corresponding elastic energy and $G_i$ the corresponding interfacial energy. Obviously, $G$ and $F_n$ are the same physical parameter, i.e.

$$F_n \equiv G \qquad (5)$$

Furthermore, $aN$ and $G_0$ are the molar free energy for 100% parent phase, thus

$$aN \equiv G_0 \qquad (6)$$

From the measurements on Cu–29% Zn–3% Al alloy by the authors [1]

$$G_c = 1.612\,T - 409.5 \quad \mathrm{J\,mol^{-1}} \qquad (7)$$

When the applied stress is zero, it is obtained from Equations 1–7 that

$$[(0.064\,51\,T - 15.33)\,m + 0.5\,m^2]\,N$$

$$\equiv (1.612\,T - 409.5)\,m + (G_e + G_i)\,m \qquad (8)$$

Assuming that $G_e$ and $G_i$ are not apparent functions of $T$, then it is obtained by comparing the coefficients of

the terms $Tm$ in both sides of Equation 8 that

$$N = 24.99 \text{ J mol}^{-1} \quad (9)$$

Thus

$$F_n = A_0 + (1.612\,T - 383.1)\,m + 12.49\,m^2 + (1.847 \times 10^{-3}\,T - 0.4858)\sigma m \quad \text{J mol}^{-1} \quad (10)$$

This is the molar free energy in the SI unit system, and it is also the free energy (density) function with dimensions.

### 3.2. Elastic energy and interfacial energy

Consider the case when the applied stress is zero and the transformation is driven only by temperature change. It is obtained from Equation 8 that

$$G_e m + G_i m = 12.49\,m^2 + 26.4\,m \quad (11)$$

that is

$$G_e + G_i = 12.49\,m + 26.4 \quad (12)$$

Although there is no way to separate $G_e$ and $G_i$ thoroughly, it is possible to discuss the functional relationships between either of them and $m$. For one mole of material, $m$ is the volume percentage and is proportional to the marteniste volume. Becuase the interfacial energy per unit area is constant, the total interfacial energy for one mole of material, $G_i m$ in Equation 11, is proportional to the total surface area of martensite. For an ordinary three-dimensional shape, the surface area is proportional to the volume to the 2/3 power. For some special shapes, for instance a cylinder with fixed bottom area or a disc with fixed height, the surface is proportional to the volume. In general, for an ordinary regular shape, the surface area is not likely to be proportional to the volume squared. Therefore, it could be deduced that the total interfacial energy $G_i m$ in Equation 11 is proportional to $m$, and the total elastic strain energy is a second-order power function of $m$. In other words, the interfacial energy caused by unit marteniste formation is constant and the corresponding elastic energy is a linear function of $m$.

Earlier investigators [5, 6], based on Eshelby's elastic theory [10] and the assumption that the martensite plate is oblate spheroidal in shape, deduced that the elastic energy $g_e$ caused by unit martensite formation is proportional to $y/r$, i.e.

$$g_e = A(y/r) \quad (13)$$

where $A$ is a constant, $Y$ is the half-thickness and $r$ the radius of the martensite plate. These investigators concluded that, for martensitic radial growth, $y/r$ decreased with increasing $r$ and then $g_e$ decreased, therefore the radial growth occurred spontaneously but not thermoelastically; and that the radial growth would be stopped only by grain boundaries or other strong obstacles. These conclusions are not consistent with the observed results in this paper and some other investigators [11] also did not agree with those conclusions. According to the viewpoint of this paper, the elastic energy caused by unit martensite formation increases linearly with increasing martensite percentage in the range of 20–70% martensite for Cu–29% Zn–3% Al alloy. Incidentally, to the authors' knowledge, no report to confirm experimentally those earlier conclusions [5, 6] has been published yet. This question has been discussed further in another paper by the authors [12].

According to the result in this paper, the interfacial energy $G_i$ caused by unit martensite formation is constant. For this result, there are at least three possible explanations. First, that as assumed by Dunne and Wayman [7] the martensite is in a thin plate shape, so that the surface area is approximately proportional to volume. The second explanation is that the self-accommodating variants advancing between parallel martensite plates have a constant surface area per unit volume. The third explanation could be that the martensites might have internal interfaces which contribute to the main part of $G_i$.

### 3.3. Friction quasi-enthalpy and quasi-entropy

According to the authors' suggestion [1], the friction caused by phase interface motion was quantitatively described by a friction function $F_r$, friction quasi-enthalpy $H_r$ and friction quasi-entropy $S_r$;

$$F_r = H_r - TS_r \quad (14)$$

$H_r$, $S_r$ and $F_r$ were expressed [1] with dimensionless values. All values in Equation 14 can be changed into SI units by the conversion factor $N$:

$$\begin{aligned} H_r &= N(-3.875 + 1.633 \times 10^{-2}\sigma)m \\ &= (-96.84 + 0.4081\,\sigma)m \quad \text{J mol}^{-1} \\ S_r &= N(0.019\,51 - 7.393 \times 10^{-5}\sigma)m \\ &= (0.4785 - 1.847 \times 10^{-3}\sigma)m \quad \text{J mol}^{-1}\,\text{K}^{-1} \end{aligned} \quad (15)$$

where $H_r$ and $S_r$ have the same units as those of enthalpy and entropy, respectively. Let $F_r$ be the (free) energy to overcome the friction caused by the interface motion, then $H_r$ and $S_r$ are the corresponding friction quasi-enthaply and friction quasi-entropy, respectively. The direct physical meanings of these are the width of the hysteresis loop and the slope difference between the segments of cooling and heating, respectively.

The thermoelastic martensitic transformations have two characteristics: reversibility and hysteresis. Some authors have introduced the concept of friction to explain the hysteresis [5, 11, 13]. In this paper, the friction is treated by introducing $H_r$ and $S_r$, which are irreversible thermodynamic functions and depend on the boundary structure, mobility, and the structures and states of the materials on both sides of the interface. The values of $H_r$ and $S_r$ may be deduced for a given boundary model and motion mode.

## 4. Conclusions

1. For Cu–29% Zn–3% Al alloy, the free-energy function $F_n$, the friction quasi-enthalpy $H_r$ and the

friction quasi-entropy $S_r$ in the SI unit system are respectively

$$F_n = A_0 + (1.612\,T - 383.1)m + 12.49\,m^2 + (1.847 \times 10^{-3}\,T - 0.4858)\sigma\,m \quad \mathrm{J\,mol^{-1}}$$

$$H_r = (-96.84 + 0.4081\,\sigma)m \quad \mathrm{J\,mol^{-1}}$$

$$S_r = (0.4785 - 1.847 \times 10^{-3}\,\sigma)m \quad \mathrm{J\,mol^{-1}\,K^{-1}}$$

2. When the applied stress is zero, the elastic strain energy $G_e$ and the interfacial energy $G_i$ caused by unit martensite formation in one mole of alloy are

$$G_e + G_i = 12.49\,m + 26.4 \quad \mathrm{J}$$

Thus, $G_i$ might be a constant and $G_e$ is a linear function of $m$:

$$G_i = C \quad \mathrm{J}$$

$$G_e = 12.49\,m + (26.4 - C) \quad \mathrm{J}$$


## Acknowledgements

This study has been supported by The Office of Naval Research, USA, and is supported by The National Natural Science Foundation of China (No. 59 071 058).


## References


1. Y. DENG and G. S. ANSELL, *Acta Metall.* **38** (1990) 69.
2. Y. DENG, Doctoral thesis, Rensselaer Polytechnic Institute, USA (1984).
3. L. KAUFMAN and M. COHEN, *Progr. Metal Phys.* **7** (1958) 165.
4. T. A. SCHROEDER and C. M. WAYMAN, *Acta Metall.* **25** (1977) 1375.
5. G. B. OLSON and M. COHEN, *Scripta Metall.* **9** (1975) 1247.
6. H. C. LING and W. S. OWEN, *Acta Metall.* **29** (1981) 1721.
7. D. P. DUNNE and C. M. WAYMAN, *Met. Trans.* **4** (1973) 147.
8. S. CHAKRAVORTY and C. M. WAYMAN, *Acta Metall.* **25** (1977) 989.
9. S. KAJIWARA and T. KIKUCHI, *ibid.* **30** (1982) 589.
10. J. D. ESHELBY, *Progr. Solid Mech.* **2** (1961) 87.
11. H. C. TONG and C. M. WAYMAN, *Scripta Metall.* **11** (1977) 341.
12. Y. DENG and G. S. ANSELL, *Acta Metall. Sinica* **26** (1990) A382. [English edition **4A** (1991) 143.].
13. I. CORNELIS and C. M. WAYMAN, *Scripta Metall.* **10** (1976) 359.



*Received 23 July 1990*
*and accepted 6 February 1991*